Structural Isomerism and Competitive Proton Solvation between Methanol and Water in $H^+(CH_3OH)_m(H_2O)_n$, $m + n = 4$†

C.-C. Wu,‡,§ C. Chaudhuri,§ J. C. Jiang,|| Y. T. Lee,‡,§ and H.-C. Chang*,§

Department of Chemistry, National Taiwan University, Taipei, Taiwan 106, Republic of China, Institute of Atomic and Molecular Sciences, Academia Sinica, P.O. Box 23-166, Taipei, Taiwan 106, Republic of China, and Department of Chemical Engineering, National Taiwan University of Science and Technology, Taipei, Taiwan 106, Republic of China

Received: July 30, 2003; In Final Form: October 30, 2003

Competitive solvation of the excess proton in protonated mixed methanol−water clusters [$H^+(CH_3OH)_m(H_2O)_n$, $m + n = 4$] has been characterized by vibrational predissociation spectroscopy in combination with density functional theory calculations. The solvation topology of the clusters can be classified as (1) the closed shell, in which a hydronium ion H_3O^+ is fully solvated by three neutral molecules forming a complete solvation shell, and (2) the open chain, where the excess proton is tugged between two mixed subunits in a linear chain. The existence of these two types of isomer is verified from a close examination of the characteristic free-OH and hydrogen-bonded-OH stretching modes in the spectra. It is found that sequential replacement of the water molecule in $H^+(H_2O)_4$ by methanol redistributes the population between the closed-shell and the open-chain isomers. While the excess proton is preferentially taken by methanol (instead of water) in the chain configuration, it can be either localized as $CH_3OH_2^+$ or delocalized as $CH_3OH\cdots H^+\cdots CH_3OH$ at $m \geq 2$, depending sensitively on the number of the methanol molecules and the symmetry of the cluster isomers. In contrast to that of $NH_4^+(NH_3)_m(H_2O)_n$, $m + n = 4$, previously studied, this work provides a clear picture of competitive solvation of a charge between the constituent solvent molecules within a cluster.

Introduction

Study of proton solvation and migration in a hydrogen-bonding network is essential to the understanding of many chemically and biologically important processes in condensed phases.[1,2] One of the motivations in the early study is to elucidate the abnormally high mobility of protons in aqueous solution, and the subject has been extensively investigated by both experiments and theories over several decades.[2−5] The widely accepted model to date is the Grötthuss mechanism,[6] where the proton migration is interpreted as a translocation of two different ion cores (the Eigen[7] and Zundel[8] cations) along the hydrogen-bonding network.[3] In the Eigen cation ($H_9O_4^+$), the hydronium ion is fully solvated by three neutral water molecules with a total coordination of three, while in the Zundel cation ($H_5O_2^+$), the excess proton is equally shared by the two neutral water molecules, allowing for a total coordination of four for outer-shell formation. The Zundel cation has been envisioned as the proton-transfer intermediate as the H_3O^+-centered structure is energetically more stable than the $H_5O_2^+$-centered structure by 0.6 kcal/mol in aqueous acids.[5a] In the gas phase, formation and reactions of the Eigen-type water clusters have been extensively studied by both experiments and theories,[9,10] whereas the Zundel-type water clusters have been rarely explored, except that of the protonated water dimer.[11,12] Recently, Jiang et al.[13] examined the infrared spectra of $H^+(H_2O)_n$ produced from a supersonic expansion in an effort to identify these two types of cation in size-selected water clusters. A comparison of experimental and computational spectra indeed provided evidence for the existence of the proton-transfer intermediate, $H_5O_2^+(H_2O)_4$, as a stable isomer of $H^+(H_2O)_6$ in the gas phase.

Methanol is another interesting model compound for the study of proton transport in hydrogen-bonding networks. In fact, the abnormally high proton mobility has also been observed in liquid methanol.[14] Unlike the water molecule, however, methanol has a hydrophobic methyl group, which terminates one of the hydrogen-bonding sites, and thereby the methyloxonium ion ($CH_3OH_2^+$) has a total coordination of two. By use of infrared spectroscopy, Chang et al.[15] identified both linear and cyclic isomers for the protonated methanol pentamer and proposed that intermolecular proton transfer can occur via a series of hydrogen bond breaking and reforming processes in this cluster. Ab initio calculations further predicted that the protonated methanol dimer $H^+(CH_3OH)_2$ possesses an inter-oxygen distance of 2.4 Å, which is substantially shorter than that (2.8 Å) of the neutral dimer. If quantum effects are taken into account, the $CH_3OH\cdots H^+\cdots CH_3OH$ (or $C_2H_9O_2^+$) form should be a better representation than $CH_3OH_2^+\cdots CH_3OH$ for the ion core. It is a structural analogue of the Zundel cation in protonated methanol clusters.

To extend our knowledge on proton solvation in hydrogen-bonding networks, we have systematically investigated the protonated mixed methanol−water clusters as the model systems. There have been a number of studies concerning the protonation site, isomeric structure, thermochemistry, and metastable decomposition of these clusters in the past.[16−22] Kebarle et al.,[16] for example, conducted thermochemical measurements and concluded that the preference for methanol does not exist in a distinct inner−outer-shell behavior for $H^+(CH_3OH)_m(H_2O)_n$ with $m + n \leq 6$. Moreover, the notation

† Part of the special issue "Fritz Schaefer Festschrift".

* Author to whom correspondence may be addressed. E-mail: hcchang@po.iams.sinica.edu.tw.

‡ National Taiwan University.

§ Institute of Atomic and Molecular Sciences.

|| National Taiwan University of Science and Technology.

10.1021/jp0309318 CCC: $27.50
Published on Web 12/24/2003

$CH_3OH_2^+(CH_3OH)_{m-1}(H_2O)_n$ or $H_3O^+(CH_3OH)_m(H_2O)_{n-1}$ does not seem to describe properly the structures of these small cluster ions. The work of Meot-Ner[18] additionally indicated that the most favored topology of $H^+(CH_3OH)_m(H_2O)_n$, with $n + m$ up to 6, would place the methanol molecules near the charge center and water molecules at the periphery. This conclusion for the preferential take-up of the proton by methanol in small-sized clusters is in accord with the positive inductive effect of the methyl group, which enhances the proton affinity of the methanol molecule.

Aside from the thermochemical measurements, metastable decomposition studies on the mixed solvent cluster ions also yield fruitful information about the clusters' structures. By determining the peak intensities of the metastable ions produced from competing decomposition channels, Stace and Shukla[17] found that the closed-shell H_3O^+-centered structure, in addition to the $CH_3OH_2^+$-centered structure, is an important form in large methanol−water clusters. This observation of the structural transformation from the $CH_3OH_2^+$-centered form to the H_3O^+-centered form is further confirmed by Castleman and co-workers[19] and Garvey and co-workers.[20] Our group has recently conducted a series of infrared spectroscopic measurements on $H^+(CH_3OH)(H_2O)_n$ and $H^+(CH_3OH)_m(H_2O)$ separately to identify isomeric structures of these cluster ions.[21,22] It is concluded that the exact position of the excess proton and the arrangement of the methanol/water molecules in them vary sensitively not only with the hydration number but also with the geometry of the cluster isomers.

We carried out in this work both infrared spectroscopic measurements and ab initio calculations for cluster ions of water/methanol binary mixtures, i.e. $H^+(CH_3OH)_m(H_2O)_n$ with $m + n = 4$. The study is undertaken to gain a better understanding of the interaction nature of selective proton solvation or, more specifically, competitive proton solvation between different solvent molecules. This is a computationally demanding task because the cluster ions to be investigated possess a large number of stable and energetically similar isomers. While the isomers studied often lack distinct spectral signatures, with the aid of density functional theory calculations, assignment of the experimental spectra and identification of different proton solvation structures have been possible.

Experimental and Computational Methods

A. Experiments. The vibrational predissociation spectra of $H^+(CH_3OH)_m(H_2O)_n$, $m + n = 4$, were obtained with an ion-trap tandem mass spectrometer coupled with a pulsed infrared laser system. Details of the apparatus have been described elsewhere and are not repeated here.[23a] In short, we produced the mixed methanol−water cluster ions using a corona discharge ion source with a backing pressure of 30−200 Torr behind a room-temperature nozzle (orifice diameter ~100 μm). The CH_3OH and H_2O vapors were premixed with proper ratios in the gas chamber using pure H_2 as the carrier gas. To produce the protonated water tetramer, $H^+(H_2O)_4$, a liquid nitrogen trap was employed to maintain low vapor pressures of water in the gas line. Supersonic expansion of the ionized and neutral gas molecules through the nozzle synthesized the cluster ions of interest. The typical temperature of the cluster ions thus produced is 170 K.[21,22]

Prior to spectroscopic measurements, the ion beam was guided, shaped, and focused by a few sets of electrostatic lenses to a magnetic sector mass filter for cluster size selection. The beam was then refocused, bent 90° by electrostatic quadrupole fields, and finally directed to an octopole ion trap for storage.

TABLE 1: Comparison of Experimental and DFT-Calculated Energies (kcal/mol) for the Clustering Reactions, $H_3O^+ + m CH_3OH + (n - 1)H_2O \rightarrow H^+(CH_3OH)_m(H_2O)_n$

	calculations[b]				experiments[c]	
isomers[a]	$-\Delta E_n$	$-\Delta H_n^{298}$	$-\Delta G_n^{298}$	$-\Delta G_n^{170}$	$-\Delta H_n^\circ$	$-\Delta G_n^\circ$
W4I	70.9	72.9	48.4	58.9	68.4	46.9
W4II	68.9	71.2	46.2	56.9		
M1W3I	73.9	75.2	50.5	61.1	76.6	53.1
M1W3II	74.0	75.5	50.3	61.1		
M1W3III	71.8	73.5	48.4	59.2		
M2W2I	76.0	77.2	50.8	62.1	79.8	56.2
M2W2II	77.1	77.9	52.5	63.4		
M2W2III	75.8	76.8	50.9	62.0		
M2W2IV	75.5	76.6	50.8	61.9		
M2W2V	74.4	75.6	49.7	60.8		
M3W1I	80.1	80.1	54.6	65.6	82.3	58.5
M3W1II	79.7	80.1	53.9	65.2		
M3W1III	78.6	79.0	53.3	64.3		
M4I	82.5	82.1	56.0	67.2	84.6	60.1

[a] Calculated isomeric structures depicted in Figure 1. [b] Using B3LYP/aug-cc-pVDZ//6-31+G* with zero-point vibrational energies corrected. [c] Reference 18.

Infrared laser pulses were introduced into the trap to pump the stored ions to their first vibrationally excited states with photon energies of 8−11 kcal/mol in the frequency range of 2700−3800 cm^{-1}. Fragmentation followed as $H^+(CH_3OH)_m(H_2O)_n + h\nu \rightarrow H^+(CH_3OH)_m(H_2O)_{n-1} + H_2O$ and $H^+(CH_3OH)_m(H_2O)_n + h\nu \rightarrow H^+(CH_3OH)_{m-1}(H_2O)_n + CH_3OH$. Only the water-loss channel was monitored for all the species except $H^+(CH_3OH)_4$. A quadrupole mass filter selected the fragment ions for detection by a Daly electrode. The detected ion intensity was recorded as a function of laser excitation frequency to obtain the infrared action spectra. Though the multicomponent system offers a good opportunity for mass-selected detection of the photofragment ions via vibrational excitation,[22] the dominant channel is still the water loss (rather than the methanol loss), which is ~2 kcal/mol more accessible.[18]

B. Computations. Ab initio calculations were carried out using the commercial Gaussian 98 package to assist interpretation of the observed spectra. The calculations, based on the density-functional theory (DFT), utilized a standard analytical gradient method.[24] We optimized the geometries of the cluster ions without imposing any symmetry constraints at the B3LYP level of computation with the 6-31+G* basis set (denoted as B3LYP/6-31+G*). Second-derivative calculations of the energy hypersurfaces supplied both harmonic vibrational frequencies and infrared absorption intensities of various structural isomers to be compared with measurements. A scaling factor of 0.973 was chosen for all the calculated OH-stretching frequencies of both water and methanol as conducted previously.[15,23]

To provide a more accurate assessment of the total interaction energies of the cluster isomers, a larger basis set (aug-cc-pVTZ) was employed in the calculations based on the geometries optimized by B3LYP/6-31+G*. Table 1 lists the results of the energy calculations (denoted as B3LYP/aug-cc-pVTZ//6-31+G*) for various low-energy isomers of $H^+(CH_3OH)_m(H_2O)_n$ with $m + n = 4$. We derived the total hydrogen-bond enthalpies and free energies of the cluster ions according to the reactions, $H_3O^+ + m CH_3OH + (n\text{-}1)H_2O \rightarrow H^+(CH_3OH)_m(H_2O)_n$, and compared them to the experimental values of Meot-Ner.[18] The stepwise replacement of H_2O by CH_3OH is seen to be exothermic for every step from the pure water tetramer to the neat methanol cluster (Table 1).

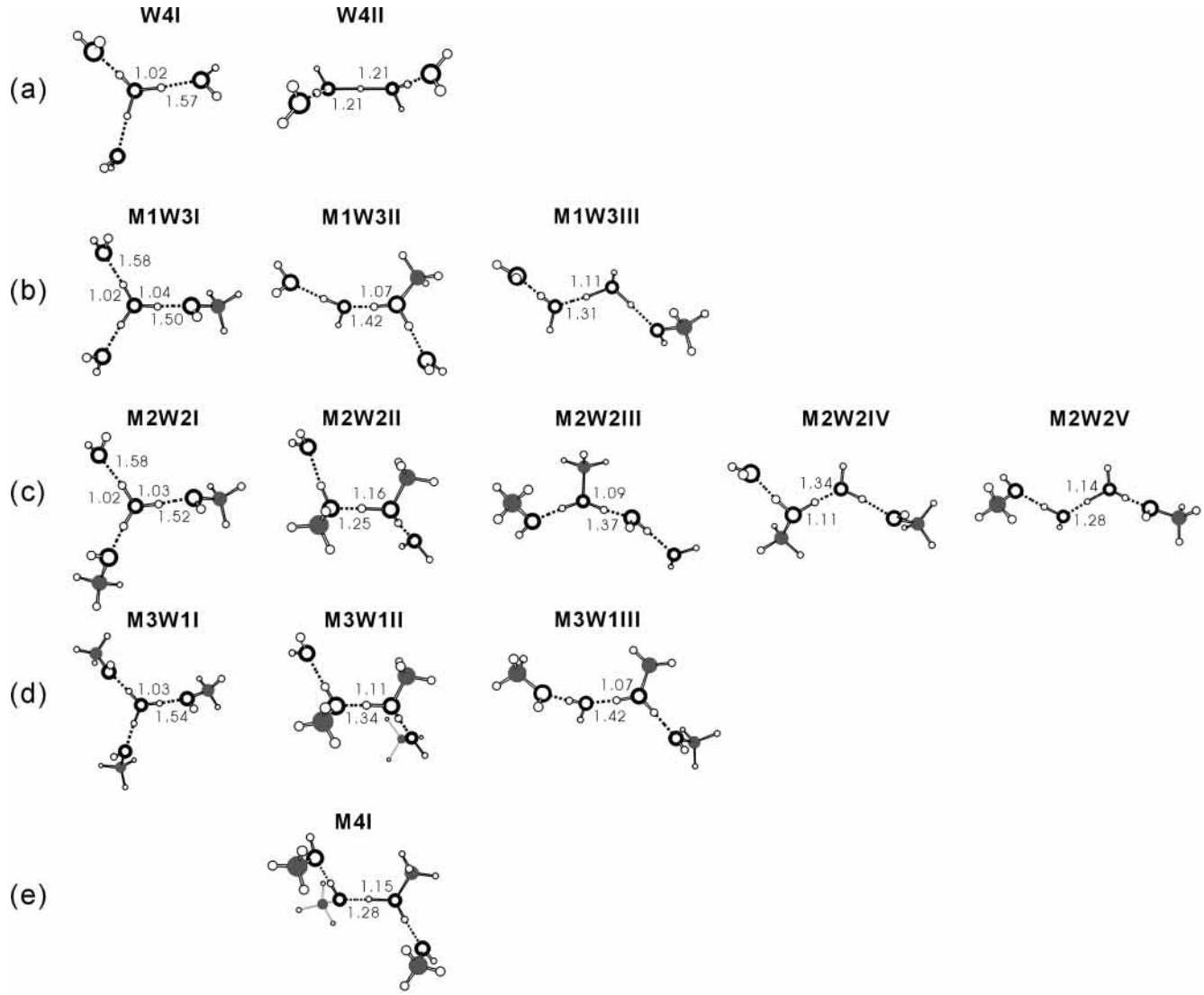

Figure 1. DFT-optimized structures of (a) $H^+(H_2O)_4$, (b) $H^+(CH_3OH)(H_2O)_3$, (c) $H^+(CH_3OH)_2(H_2O)_2$, (d) $H^+(CH_3OH)_3(H_2O)$, and (e) $H^+(CH_3OH)_4$. The C, O, and H atoms are denoted by solid gray spheres, large open spheres, and small open spheres, respectively. The bond lengths are all given in units of Å.

Results and Analysis

Figure 1 shows the structures of low-energy isomers of $H^+(CH_3OH)_m(H_2O)_n$, $m + n = 4$, optimized by the B3LYP/6-31+G* calculation. The experimental spectra of the corresponding clusters are displayed in Figure 2, showing the consecutive spectral changes (parts a → e) as a result of the sequential replacement of water in $H^+(H_2O)_4$ by methanol. Figure 3 provides a comparison between the observed and the DFT-calculated spectra of the individual stable isomers for each cluster ion. From Figure 1, one may roughly classify the proton solvation modes as (1) the closed-shell (branched) form, where the H_3O^+ ion is fully solvated by the solvent molecules and (2) the open-chain (linear) form, where the four solvent molecules are randomly combined as two dimer pairs competing for the excess proton. As will be shown in the followings, the Zundel-like cations can be stabilized through introduction of the methyl groups and they can be fairly well identified with IR spectroscopy and DFT calculations as the diagnostic tools.

A. $m = 0$, $n = 4$. The experimental spectrum and the calculated stick diagrams of the pure protonated water tetramer $H^+(H_2O)_4$ are presented in Figures 2a and 3a. Two distinct absorption bands at 3733 and 3644 cm^{-1} were obtained, and they are attributed, respectively, to the asymmetric and symmetric OH stretches (denoted as a-OH_2 and s-OH_2) of the first-shell water molecules acting as single proton acceptors (denoted as 1° H_2O(A)). The sharpness of the features implies that all the 1° H_2O molecules own similar environments. Compared to the Eigen cation (**W4I**), the Zundel-type isomer (**W4II**) containing the excess proton equally shared by the water dimer pairs is higher in energy by 2.0 kcal/mol (in terms of $-\Delta E_n$ here and hereinafter). Moreover, the absorption bands ascribable to the free-OH stretches (denoted as f-OH_W) of the two single-acceptor−single-donor (AD) H_2O in **W4II** are absent in the spectrum. The results clearly lead us to the identification of isomer **W4I** in the corona-discharged supersonic expansion.

No absorption was detectable in this experiment for the bonded-OH stretches in the frequency range 2700−3600 cm^{-1}. Price et al.[25] have previously observed a very weak feature at ~2700 cm^{-1} and assigned it to the hydrogen-bonded OH stretches of the H_3O^+ ion core. An explanation for the weakness of this feature is that the photon energy ($h\nu \approx 8$ kcal/mol) used in this regime is much lower than that required to cross over the dissociation barrier, $\Delta H_D° = 17.6$ kcal/mol,[26] thereby limiting the efficiency of detaching 1° H_2O from H_3O^+ by the infrared laser.

B. $m = 1$, $n = 3$. Replacement of one water molecule in

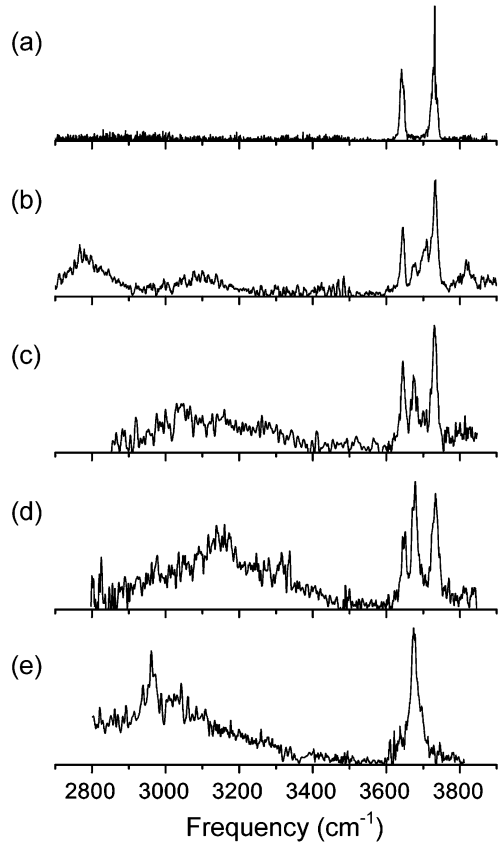

Figure 2. Comparison of the power-normalized vibrational predissociation spectra of (a) $H^+(H_2O)_4$, (b) $H^+(CH_3OH)(H_2O)_3$, (c) $H^+(CH_3OH)_2(H_2O)_2$, (d) $H^+(CH_3OH)_3(H_2O)$, and (e) $H^+(CH_3OH)_4$ at the same cluster temperature of ~170 K.

$H^+(H_2O)_4$ by methanol markedly changes the observed spectrum. Fruitful information about the ion core is revealed from the four free-OH stretches at 3600−3800 cm^{-1} (Figure 2b). In addition to the a-OH_2 and s-OH_2 bands as observed for $H^+(H_2O)_4$, two new features emerge at 3706 and 3673 cm^{-1} and they can be associated with the f-OH_W of H_2O(AD) and the f-OH_M of CH_3OH(A), respectively.[13,15] Figure 3b compares the experimental spectrum with the DFT-calculated stick spectra of three low-energy isomers, **M1W3I**−**M1W3III** (Figure 1b). Identification of both **M1W3I** (H_3O^+ centered) and **M1W3II** ($CH_3OH_2^+$ centered), instead of either one of them, allows us to properly reproduce the observed spectrum in the free-OH stretch region (Figure 4a). We rule out the possibility for the presence of isomer **M1W3III** in the beam, not only because the calculated spectrum fails to match with the observed spectrum but also because it is less stable than the lowest-energy isomer **M1W3II** by 2.2 kcal/mol. Further assignments of the corresponding absorption bands in the bonded-OH stretching region are given in Table 2.[21]

The cluster ion $H^+(CH_3OH)(H_2O)_3$ is unique in that it provides distinct spectral fingerprints (i.e., f-OH_W and f-OH_M) for identification of isomers. This uniqueness is well illustrated in Figure 3b, where we resolve the isomeric structures of the cluster and confirm the coexistence of H_3O^+-centered and $CH_3OH_2^+$-centered forms in the supersonic expansion. One may further estimate the relative population of **M1W3I** and **M1W3II** in the beam by comparing the observed band intensities to the calculated values of f-OH_W and f-OH_M on the premise that the dissociation probability is the same for both cluster isomers upon infrared laser excitation in the free-OH region. Shown in Figure 4a are the spectral features of a-OH_2, s-OH_2, f-OH_W, and f-OH_M, simulated individually with four Gaussian profiles with their bandwidths adjusted to fit the experimental values. We obtained a population ratio of roughly 1:1, suggesting that both isomers (**M1W3I** and **M1W3II**) are nearly equally populated in the beam. Interestingly, this ratio is in good agreement with the result of the DFT calculation, which predicts a free energy difference ($\Delta\Delta G_n^{170}$) of less than 0.1 kcal/mol between these two isomeric forms at 170 K (Table 1). However, this agreement should be considered fortuitous because the error involved in the relative-energy calculation is much larger than this energy difference, typically in the range of ±0.5 kcal/mol.

Despite the fact that the spectrum displayed in Figure 3b provides convincing evidence for the coexistence of isomers in the beam, the lack of symmetry of the cluster ion prevents us from identifying isomer **M1W3III** containing a Zundel-type ion core. Nonetheless, it is noticed from the calculations that the energy difference between the closed-shell form and the open-chain isomer decreases significantly from 2.0 kcal/mol of $H^+(H_2O)_4$ to 0.1 kcal/mol of $H^+(CH_3OH)(H_2O)_3$ owing to the replacement of water by methanol (Table 1). Further replacement of the water molecule by one more methanol subunit is expected to restore the symmetry (an odd−even effect) and lead to formation of the unusual proton delocalization structure (−O•••H^+•••O−).

C. *m* = 2, *n* = 2. Given in Figure 1c are the low-energy structures of the $H^+(CH_3OH)_2(H_2O)_2$ isomers. Among them, the isomer **M2W2II**, containing a CH_3OH•••H^+•••CH_3OH ion core with two water molecules at the periphery, is lowest in energy. Interestingly, the proton in this core is situated nearly in the middle between the two oxygen atoms, with an −O••• H^+ bond length of r_{OH^+} = 1.16 and 1.25 Å, respectively. As found in our previous work for $H^+(CH_3OH)_4$ and $H^+[(CH_3)_2O](H_2O)_2$,[15,27] the potential well along this proton transfer coordinate is quite flat. The proton is essentially delocalized between these two methanol subunits with a vibrationally averaged bond length of $\langle r_{OH^+}\rangle$ = 1.21 Å due to the zero-point energy effect. This isomer, containing a symmetric ionic hydrogen bond, is a structural analogue of the Zundel-type water cluster, $H_5O_2^+(H_2O)_4$.[13]

The DFT-calculated stick spectra of $H^+(CH_3OH)_2(H_2O)_2$ isomers are compared closely with the experimental spectrum in Figure 3c. In line with our expectation, the diversity of the configurations (cf. Figure 1c) makes the structural identification of $H^+(CH_3OH)_2(H_2O)_2$ very difficult even though we narrow our prediction to only the chain structures. If we arrange the excess proton (H^+), the methanol molecule (M), and the water molecule (W) randomly in the linear chain, four combinations are derived, WMH^+MW (**M2W2II**), MMH^+WW (**M2W2III**), WMH^+WM (**M2W2IV**), and MWH^+WM (**M2W2V**). Note that isomer **M2W2V**, which contains two methanol molecules at the periphery, is highest in energy among the four combinations. It is 2.7 kcal/mol less stable than its structural counterpart **M2W2II**. This result is anticipated because methanol has a proton affinity (PA) of 281 kcal/mol, higher than that of water by 15 kcal/mol,[28] thereby energetically favoring the formation of **M2W2II**.

In determination of the topology of the cluster isomers produced in the supersonic expansion, the spectral signatures f-OH_W and f-OH_M are the key indicators. Out of the four characteristic free-OH stretching bands observed for $H^+(CH_3OH)(H_2O)_3$, the f-OH_W of $H^+(CH_3OH)_2(H_2O)_2$ can be barely found in Figure 2c, indicating that the population of both **M2W2III** and **M2W2IV** in the beam is low. The f-OH_M band, in contrast, is distinct at 3676 cm^{-1}, suggesting a high abundance

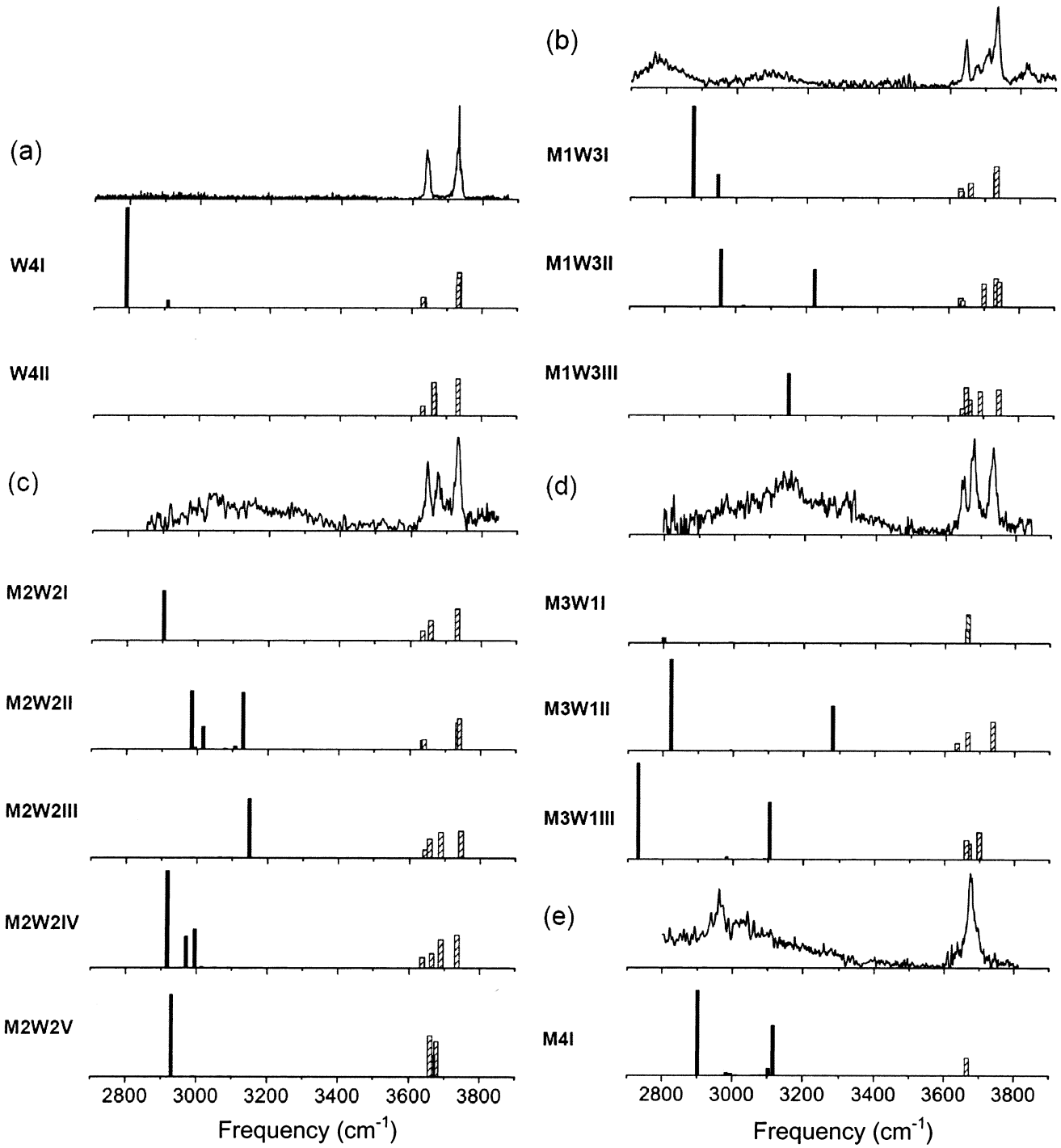

Figure 3. Comparison of the power-normalized vibrational predissociation spectra of (a) $H^+(H_2O)_4$, (b) $H^+(CH_3OH)(H_2O)_3$, (c) $H^+(CH_3OH)_2(H_2O)_2$, (d) $H^+(CH_3OH)_3(H_2O)$, and (e) $H^+(CH_3OH)_4$ at 170 K with the corresponding DFT-calculated stick diagrams of isomers depicted in Figure 1. The calculated intensities of the free-OH stretches (slashed bars) are amplified by a factor of 5 for clearer comparison to those of the bonded-OH stretches (solid bars).

of the second-lowest-energy isomer **M2W2I** in the beam (Figure 3c). This isomer, similar to **M1W3I**, is H_3O^+ centered but with the ion fully solvated by two methanol and one water molecules. It is ~1 kcal/mol higher in energy than the global minimum **M2W2II**, which, unfortunately, lacks distinguishable free-OH stretching features for identification. Nevertheless, the coexistence of these two isomers can be revealed from a close comparison of the relative intensities of the free-OH stretching features between the experimental and calculated spectra. Only with the **M2W2II** included to enhance the intensities of both the a-OH_2 and s-OH_2 bands can the observed spectrum be properly reproduced (cf. Figure 4b). The best estimates of the population percentage match closely with 40 and 60% for isomers **M2W2I** and **M2W2II**, respectively.

D. $m = 3, n = 1$. Comparison of the calculated stick diagrams to the experimental spectrum of $H^+(CH_3OH)_3(H_2O)$ is given in Figure 3d. The observed absorption bands at 3733, 3677, and 3647 cm^{-1} in the free-OH stretching region are all similar to those of $H^+(CH_3OH)_2(H_2O)_2$ except that the intensity of the f-OH_M mode markedly increases. While isomer **M3W1II** displays all the required a-OH_2, s-OH_2, and f-OH_M stretching features, isomer **M3W1I** shows only the f-OH_M band and is close to **M3W1II** within 0.4 kcal/mol in energy (Table 1). The fingerprint (f-OH_W) of isomer **M3W1III**, which is less stable

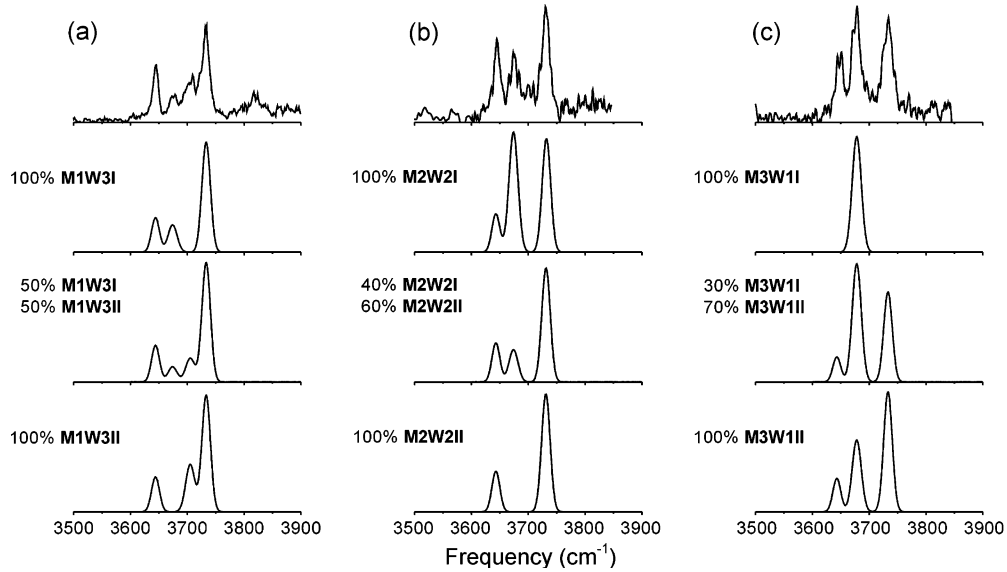

Figure 4. Simulations of the experimental spectra of (a) $H^+(CH_3OH)(H_2O)_3$, (b) $H^+(CH_3OH)_2(H_2O)_2$, and (c) $H^+(CH_3OH)_3(H_2O)$ based on the computed stick spectra of isomers **M1W3I** and **M1W3II**, **M2W2I** and **M2W2II**, and **M3W1I** and **M3W1II**. All the spectral features are fitted with Gaussian profiles, with their bandwidths adjusted to the experimental values of 15, 14, 16, and 16 cm^{-1} for a-OH_2, s-OH_2, f-OH_W, and f-OH_M stretches, respectively. The numbers given on the left are the contributions of the individual isomers to establishing the best fit of the experimental spectra.

TABLE 2: Frequencies (cm^{-1}) and Assignments of the Observed OH Stretching Features of $H^+(CH_3OH)_m(H_2O)_n$, $m + n = 4$

species	frequency	isomers[a]	assignments[b]
$H^+(H_2O)_4$	3733	**W4I**	a-OH_2 of 1° H_2O(A)
	3644	**W4I**	s-OH_2 of 1° H_2O(A)
$H^+(CH_3OH)(H_2O)_3$	3733	**M1W3I, M1W3II**	a-OH_2 of 1° & 2° H_2O(A)
	3706	**M1W3II**	f-OH of 1° H_2O(AD)
	3673	**M1W3I**	f-OH of 1° CH_3OH(A)
	3644	**M1W3I, M1W3II**	s-OH_2 of 1° & 2° H_2O(A)
	3091	**M1W3II**	bonded-OH of 1° H_2O(AD)
	2783	**M1W3I, M1W3II**	bonded-OH of $CH_3OH_2^+$ & H_3O^+
$H^+(CH_3OH)_2(H_2O)_2$	3731	**M2W2I, M2W2II**	a-OH_2 of 1° & 2° H_2O(A)
	3676	**M2W2I**	f-OH of 1° CH_3OH(A)
	3644	**M2W2I, M2W2II**	s-OH_2 of 1° & 2° H_2O(A)
	3153	**M2W2II**	bonded-OH of 1° CH_3OH(AD)
	3047	**M2W2I, M2W2II**	bonded-OH of $CH_3OH_2^+$ and H_3O^+
$H^+(CH_3OH)_3(H_2O)$	3733	**M3W1II**	a-OH_2 of 2° H_2O(A)
	3677	**M3W1I, M3W1II**	f-OH of 1° CH_3OH(A)
	3647	**M3W1II**	s-OH_2 of 2° H_2O(A)
	3150	**M3W1II**	bonded-OH of 1° CH_3OH(AD)
$H^+(CH_3OH)_4$	3677	**M4I**	f-OH of 1° CH_3OH(A)
	2982	**M4I**	bonded-OH of $CH_3OH_2^+$

[a] Calculated isomeric structures depicted in Figure 1. [b] Notations describing the forms of hydrogen bonding for water and/or methanol molecules in the first (1°) and second (2°) solvation shells are single-acceptor (A), single-acceptor−single-donor (AD), asymmetric free-OH stretch of water (a-OH_2), symmetric free-OH stretch of water (s-OH_2), and free-OH stretch of water or methanol (f-OH).

than the minimum-energy isomer by 1.5 kcal/mol, is not found in the spectrum. It is noted that in Figure 3d, the observed intensity of the f-OH_M mode is substantially higher than those of the a-OH_2 and s-OH_2, contrary to that predicted for **M3W1II**. Again, the discrepancy in the intensity between the experimental spectrum and the computed spectrum of **M3W1II** alone is prominent, indicating the coexistence of two isomers in the beam as well. A satisfactory reproduction of the experimental features using the calculated spectra of isomers **M3W1I** and **M3W1II** is shown in Figure 4c, where the ratio of the population between **M3W1I** and **M3W1II** is estimated to be roughly 1:2. Compared to the ratio of 1:1 for **MW3I** and **M1W3II** of $H^+(CH_3OH)(H_2O)_3$ (Figure 4a), it suggests a population redistribution from the closed-shell isomer to the open-chain isomer as the number of the methanol molecule increases.

In isomer **M3W1II**, the lengths of the two $-O\cdots H^+$ bonds sharing the same H^+ are calculated to be 1.34 and 1.11 Å. These two bond lengths significantly differ, indicating that the proton is preferentially taken by one of the methanol molecules rather than being equally shared by two methanol units as in **M2W2II** (cf. parts c and d of Figure 1). This occurs because the symmetry of the cluster ion breaks down again as the numbers of the methanol and water molecules in this cluster are both odd. Interestingly, the absence of the f-OH_W signature in the spectrum helps us to conclude that the water molecule resides at the periphery as $WM\cdots H^+MM$ (**M3W1II**), rather than sitting inside as $MW\cdots H^+MM$ (**M3W1III**), in the observed open-chain isomer.

E. $m = 4$, $n = 0$. Figures 2e and 3e show the spectra of $H^+(CH_3OH)_4$. Only one intense absorption band at 3677 cm^{-1} and one broad feature spanning from 2800 to 3200 cm^{-1} were observed in the spectrum. Again, the former corresponds to the f-OH_M of 1° CH_3OH(A) residing at two ends of the linear chain. The good agreement between the observation and the calculation for **M4I** corroborates the suggestion that only this isomer was produced in the supersonic expansion. No evidence for the

formation of ring isomers was found for this cluster at an estimated internal temperature of ~170 K.[15,21,22]

Similar to **M2W2II**, isomer **M4I** contains a delocalized proton. Although the two calculated bond lengths (1.15 Å and 1.28 Å) of $-O\cdots H^+$ slightly differ in this DFT-optimized structure, a scan of the potential-energy surface along the r_{OH^+} coordinate revealed that the proton-transfer barrier vanishes when the zero-point vibrational energy is taken into account in the calculation.[15] The $CH_3OH\cdots H^+\cdots CH_3OH$ is a better representation than $CH_3OH_2^+$ in describing the ion core in this open-chain isomer.

Discussion

Among the many different ways of studying competitive proton solvation in pure and/or mixed solvent clusters, infrared spectroscopy in combination with ab initio calculations clearly is the most effective approach. The efficacy of this hybrid approach has been demonstrated in the early experiments of Yeh et al.[11] and calculations of Schaefer and co-workers[12] in the identification of $H_5O_2^+$ isolated in the gas phase. The same method has also proven successful in the study of the competitive solvation of alkali metal ions between polar and nonpolar ligands in $K^+(C_6H_6)_m(H_2O)_n$.[29] For the competitive solvation of H^+ as studied herein, several relevant cluster systems $H^+(L)_m(H_2O)_n$ have been investigated in the past.[16−23,30−36] In the cases of $m = 1$ and $L = (CH_3)_2O$, the competition of the ligand with H_2O for the excess proton has been shown to depend sensitively on the hydration number.[27] Migration of the proton from the inert solvent to water starts at $n = 2$ and completes at $n = 3$. This intriguing behavior, as first proposed by Grimsrud and Kebarle,[30a] can be identified very clearly by infrared spectroscopy because dimethyl ether is relatively inert (with a PA higher than that of water by only 27 kcal/mol) and has a coordination number (n_c) of 1 after protonation. It is in sharp contrast to that of $L = NH_3$, which is extremely active in competing for the excess proton, and consequently, NH_4^+ has been the only ion core found in $H^+(NH_3)(H_2O)_{3-6}$ and $H^+(NH_3)_m(H_2O)_n$ with $m + n = 4$.[23,25] We have attributed the observations to the fact that NH_3 has a PA much higher than that of H_2O (204 kcal/mol vs 165 kcal/mol),[28] together with the fact that NH_4^+ has a coordination number of $n_c = 4$, exceeding $n_c = 3$ of H_3O^+. With such a high coordination number, the NH_4^+ ion can prevail even when ammonia is surrounded by ligands with higher proton affinities.[37]

Between the two extreme cases, $(CH_3)_2O$ and NH_3, lies CH_3OH. The molecule has a PA higher than that of H_2O by only 15 kcal/mol. This energy difference is sufficiently small to be compensated easily by grouping water molecules on one side of the ion core, raising the PA of the water cluster to more than 193 kcal/mol.[28] However, in the case of $H^+(CH_3OH)_m(H_2O)_n$, this does not mean that the water molecules will always take the proton because the coordination number of $CH_3OH_2^+$ is 2, unlike $n_c = 1$ of $(CH_3)_2OH^+$. As a result, there is a proton pulling exerted on either side of the $-OH_2^+$ moiety and the exact position of the proton depends sensitively on the proton affinities of these two hydrogen-bonded subunits. Hence, very subtle proton-transfer reactions can occur within this mixed methanol−water cluster system.

We identify in this work two different types of structure for $H^+(CH_3OH)_m(H_2O)_n$, $m + n = 4$, from a close examination of the vibrational predissociation spectra shown in Figures 2 and 3. The closed-shell (or branched) forms all contain an H_3O^+ ion fully solvated by three neutral molecules. The open-chain (linear) forms, on the other hand, contain a proton tugged by two dimeric subunits; they are WW/WW in **W4II**, WW/MW in **W1M3II**, WM/MW in **W2M2II**, WM/MM in **W3M1II**, and MM/MM in **M4I**. From the gradual increase in the intensity of the f-OH_M band relative to those of a-OH_2 and s-OH_2 (part a → c of Figure 4), it is suggested that sequential replacement of the water molecule by methanol would switch the solvation topology from the branched form to the linear form. The figures illustrate an intriguing structural change as a result of the competitive solvation of the excess proton in the mixed solvent clusters.

The five open-chain isomers (**W4II**, **W1M3II**, **W2M2II**, **W3M1II**, and **M4I**) depicted in Figure 1 are all similar in structure; however, the position of the excess proton in them markedly varies. Particularly noteworthy is that the proton moves back and forth as the water molecules are sequentially replaced by methanol. The absolute value of the bond-length difference between these two $-O\cdots H^+$ moieties, as indicated in Figure 1, alternates as $|\Delta r_{OH^+}| = 0.00$, 0.35, 0.09, 0.23, to 0.13 Å from ($m = 0$, $n = 4$) to ($m = 4$, $n = 0$), according to the B3LYP/6-31+G* calculation. In **M1W3II** and **M3W1II**, the proton is confined at a site close to CH_3OH, forming a $CH_3OH_2^+$ ion core, while in **M2W2II** and **M4I**, the proton is effectively delocalized, bridging these two CH_3OH units in a form of $CH_3OH\cdots H^+\cdots CH_3OH$ owing to the zero-point vibrational effect. It shows an interesting odd−even effect; in particular, when the excess proton is solvated by an even number of methanol molecules in $H^+(CH_3OH)_m(H_2O)_n$ with $m + n = 4$, proton delocalization will come to play in isomers with a symmetric open-chain configuration.

An additional intriguing feature that can be found in the calculations is the effect of proton pulling between the dimeric subunits in the open-chain isomers. For $H^+(CH_3OH)_2(H_2O)_2$ as an example, there are 4 different combinations for the arrangement of methanol and water molecules in this cluster, WM/MW (**M2W2II**), MM/WW (**M2W2III**), WM/WM (**M2W2IV**), and MW/WM (**M2W2V**). Again, the lengths of the $-O\cdots H^+$ bonds vary markedly with the arrangement of the W and M moieties. As expected, the proton lies at a site close to the middle between these two dimeric subunits in **M2W2II** ($|\Delta r_{OH^+}| = 0.09$ Å) and **M2W2V** ($|\Delta r_{OH^+}| = 0.14$ Å), both of which are symmetric in the W/M arrangement, whereas the proton is preferentially taken by the methanol dimer subunit in **M2W2III** with $|\Delta r_{OH^+}| = 0.28$ Å. Somewhat surprising is that the proton is predicted to situate at a site much closer to the methanol than the water molecule in **M2W2IV** ($|\Delta r_{OH^+}| = 0.23$ Å), which has an arrangement of WM/WM. The result, however, is in qualitative agreement with the fact that the proton binds more strongly with methanol than water.

Conclusion

We have presented a case, $H^+(CH_3OH)_m(H_2O)_n$ with $m + n = 4$, in which systematic investigations of the cluster ions have been made using a combined technique of infrared spectroscopy and ab initio calculations. Two types of isomer (closed-shell and open-chain forms) are identified from a close analysis of the characteristic absorption bands of water and methanol in both the free-OH and hydrogen-bonded-OH stretch regions at 2700−3900 cm^{-1} for the mixed solvent clusters. Distribution of the populations between these two isomers is observed to switch from the closed-shell H_3O^+-centered form to the open-chain $CH_3OH_2^+$-centered form as the number of the methanol molecule increases. In the chain configuration, intriguing proton pulling between the dimeric subunits (MM, WM, MW, and WW) occurs; it produces either a proton-localized ion core as

$CH_3OH_2^+$ or a proton-delocalized ion core as $CH_3OH\cdots H^+\cdots CH_3OH$. Whichever dominates depends sensitively on the number of the methanol/water molecules and the symmetry of the cluster isomers. Such an intriguing proton-pulling behavior is expected to be found in competitive solvation of the excess proton, leading to proton transfer between ligands and solvent molecules, in aqueous solutions[1] and in complex biological systems as well.[38]

Acknowledgment. We thank the Academia Sinica and the National Science Council (Grant No. NSC 92-2113-M-001-047) of Taiwan, the Republic of China, for financial support of this work.

References and Notes

(1) Marcus, Y. *Ion Solvation*; Wiley: New York, 1985.

(2) Zundel, G. *Adv. Chem. Phys.* **2000**, *111*, 1.

(3) Tuckerman, M.; Laasonen, K.; Sprik, M.; Parrinello, M. *J. Chem. Phys.* **1995**, *103*, 150. (b) Marx, D.; Tuckerman, M. E.; Hutter, J.; Parrinello, M. *Nature* **1999**, *397*, 601.

(4) Schmitt, U. W.; Voth, G. A. *J. Phys. Chem. B* **1998**, *102*, 5547. (b) Schmitt, U. W.; Voth, G. A. *Isr. J. Chem.* **1999**, *39*, 483.

(5) Agmon, N. *Chem. Phys. Lett.* **1995**, *244*, 456. (b) Agmon, N. *Isr. J. Chem.* **1999**, *39*, 493 and references therein.

(6) von Grötthuss, C. J. D. *Ann. Chim. (Paris)* **1806**, *LVIII*, 54.

(7) Eigen, M.; Maeyer, L. D. *Proc. R. Soc. London, Ser. A* **1957**, *247*, 505.

(8) Zundel, G.; Metzger, H. Z. *Phys. Chem.* **1968**, *58*, 225.

(9) Niedner-Schatteburg, G.; Bondybey, V. E. *Chem. Rev.* **2000**, *100*, 4059.

(10) Kochanski, E.; Kelterbaum, R.; Klein, S.; Rohme, M. M.; Rahmouni, A. *Adv. Quantum Chem.* **1997**, *28*, 273.

(11) Yeh, L. I.; Okamura, M.; Myers, J. D.; Price, J. M.; Lee, Y. T. *J. Chem. Phys.* **1989**, *91*, 7319. (b) Yeh, L. I.; Lee, Y. T.; Hougen, J. T. *J. Mol. Spectrosc.* **1994**, *164*, 473.

(12) Xie, Y.; Remington, R. B.; Schaefer, H. F. *J. Chem. Phys.* **1994**, *101*, 4878. (b) Valeev, E. F.; Schaefer, H. F. *J. Chem. Phys.* **1998**, *108*, 7197.

(13) Jiang, J. C.; Wang, Y.-S.; Chang, H.-C.; Lin, S. H.; Lee, Y. T.; Niedner-Schatteburg, G.; Chang, H.-C. *J. Am. Chem. Soc.* **2000**, *122*, 1398.

(14) Morrone, J. A.; Tuckerman, M. *J. Chem. Phys.* **2002**, *117*, 4403.

(15) Chang, H.-C.; Jiang, J. C.; Lin, S. H.; Lee, Y. T.; Chang, H.-C. *J. Phys. Chem. A* **1999**, *103*, 2941. (b) Chang, H.-C.; Jiang, J. C.; Chang, H.-C.; Wang, L. R.; Lee, Y. T. *Isr. J. Chem.* **1999**, *39*, 231.

(16) Kebarle, P.; Haynes, R. N.; Collins, J. G. *J. Am. Chem. Soc.* **1967**, *89*, 5753.

(17) Stace, A. J.; Shukla, A. K. *J. Am. Chem. Soc.* **1982**, *104*, 5314.

(18) Meot-Ner, M. *J. Am. Chem. Soc.* **1986**, *108*, 6189.

(19) Wei, S.; Tzeng, W. B.; Keesee, R. G.; Castleman, A. W., Jr. *J. Am. Chem. Soc.* **1991**, *113*, 1960. (b) Shi, Z.; Wei, S.; Ford, J. V.; Castleman, A. W., Jr. *Chem. Phys. Lett.* **1992**, *200*, 142.

(20) Herron, W. J.; Coolbaugh, M. T.; Vaidyanathan, G.; Peifer, W. R.; Garvey, J. F. *J. Am. Chem. Soc.* **1992**, *114*, 3684. (b) Lyktey, M. M. Y.; DeLeon, R. L.; Shores, K. S.; Furlani, T. R.; Garvey, J. F. *J. Phys. Chem. A* **2000**, *104*, 5197.

(21) Wu, C.-C.; Jiang, J. C.; Boo, D. W.; Lin, S. H.; Lee, Y. T.; Chang, H.-C. *J. Chem. Phys.* **2000**, *112*, 176.

(22) Chaudhuri, C.; Jiang, J. C.; Wang, X.; Lee, Y. T.; Chang, H.-C. *J. Chem. Phys.* **2000**, *112*, 7279. (b) Jiang, J. C.; Chaudhuri, C.; Lee, Y. T.; Chang, H.-C. *J. Phys. Chem. A* **2002**, *106*, 10937.

(23) Wang, Y.-S.; Chang, H.-C.; Jiang, J. C.; Lin, S. H.; Lee, Y. T.; Chang, H.-C. *J. Am. Chem. Soc.* **1998**, *120*, 8777. (b) Chang, H.-C.; Wang, Y. S.; Lee, Y. T.; Chang, H.-C. *Int. J. Mass Spectrom.* **1998**, *1781*, 4443.

(24) Frisch, M. J.; Trucks, G. W.; Schlegel, H. B.; Scuseria, G. E.; Robb, M. A.; Cheeseman, J. R.; Zakrzewski, V. G.; Montgomery, J. A., Jr.; Stratmann, R. E.; Burant, J. C.; Dapprich, S.; Millam, J. M.; Daniels, A. D.; Kudin, K. N.; Strain, M. C.; Farkas, O.; Tomasi, J.; Barone, V.; Cossi, M.; Cammi, R.; Mennucci, B.; Pomelli, C.; Adamo, C.; Clifford, S.; Ochterski, J.; Petersson, G. A.; Ayala, P. Y.; Cui, Q.; Morokuma, K.; Malick, D. K.; Rabuck, A. D.; Raghavachari, K.; Foresman, J. B.; Cioslowski, J.; Ortiz, J. V.; Stefanov, B. B.; Liu, G.; Liashenko, A.; Piskorz, P.; Komaromi, I.; Gomperts, R.; Martin, R. L.; Fox, D. J.; Keith, T.; Al-Laham, M. A.; Peng, C. Y.; Nanayakkara, A.; Gonzalez, C.; Challacombe, M.; Gill, P. M. W.; Johnson, B. G.; Chen, W.; Wong, M. W.; Andres, J. L.; Head-Gordon, M.; Replogle, E. S.; Pople, J. A. *Gaussian 98*, revision A.5; Gaussian, Inc.: Pittsburgh, PA, 1998.

(25) Crofton, M. W.; Price, J. M.; Lee, Y. T. In *Clusters of Atoms and Molecules*; Haberland, H., Ed.; Springer-Verlag: Berlin, 1994; Vol. II, p 44. (b) Price, J. M. Ph.D. Thesis, University of California, Berkeley, CA, 1990, Chapters 2 and 4.

(26) Meot-Ner, M.; Speller, C. V. *J. Phys. Chem.* **1986**, *90*, 6616.

(27) Chang, H.-C.; Jiang, J. C.; Hahndorf, I.; Lin. S. H.; Lee, Y. T.; Chang, H.-C. *J. Am. Chem. Soc.* **1999**, *121*, 4443.

(28) Hunter, E. P. L.; Lias, S. G. *J. Phys. Chem. Ref. Data* **1998**, *27*, 413.

(29) Cabarcos, O. M.; Weinheimer, C. J.; Lisy, J. M. *J. Chem. Phys.* **1998**, *108*, 5151. (b) Cabarcos, O. M.; Weinheimer, C. J.; Lisy, J. M. *J. Chem. Phys.* **1999**, *110*, 8429.

(30) Grimsrud, E. P.; Kebarle, P. *J. Am. Chem. Soc.* **1973**, *95*, 7939. (b) Hiraoka, K.; Grimsrud, E. P.; Kebarle, P. *J. Am. Chem. Soc.* **1974**, *96*, 3359.

(31) Stace, A. J.; Moore, C. *J. Phys. Chem.* **1982**, *86*, 3681.

(32) Deakyne, C. A.; Meot-Ner, M.; Campbell, C. L.; Hughes, M. G.; Murphy, S. P. *J. Chem. Phys.* **1986**, *84*, 4958.

(33) Iraqi, M.; Lifshitz, C. *Int. J. Mass Spectrom. Ion Processes* **1986**, *71*, 245.

(34) Mestdagh, J. M.; Binet, A.; Sublemontier, O. *J. Phys. Chem.* **1989**, *93*, 8300.

(35) Selegu, T. J.; Cabarcos, O. M.; Lisy, J. M., *J. Chem. Phys.* **1994**, *100*, 4790. (b) Weinheimer, C. J.; Lisy, J. M. *Chem. Phys.* **1998**, *239*, 357.

(36) Wisniewski, E. S.; Hershberger, M. A.; Castleman, A. W., Jr. *J. Chem. Phys.* **2002**, *116*, 5738.

(37) Wei, S.; Tzeng, W. B.; Keesee, R. G.; Castleman, A. W., Jr. *J. Am. Chem. Soc.* **1991**, *113*, 1960. (b) Wei, S.; Tzeng, W. B.; Castleman, A. W., Jr. *J. Phys. Chem.* **1991**, *95*, 585.

(38) For some representative articles, see: (a) Doyle, D. A.; Carbral, J. M.; Pfuetzner, R. A.; Kuo, A.; Gulbis, J. M.; Cohen, S. L.; Chait, B. T.; MacKinnon, R. *Sci.* **1998**, *280*, 69. (b) Green, M. E. *J. Phys. Chem. B* **2001**, *105*, 5298.